Measurement of Upper Limits for $\Upsilon \to \gamma + \mathcal{R}$ Decays*

J. L. Rosner,[1] N. E. Adam,[2] J. P. Alexander,[2] K. Berkelman,[2] D. G. Cassel,[2] J. E. Duboscq,[2] K. M. Ecklund,[2] R. Ehrlich,[2] L. Fields,[2] R. S. Galik,[2] L. Gibbons,[2] R. Gray,[2] S. W. Gray,[2] D. L. Hartill,[2] B. K. Heltsley,[2] D. Hertz,[2] C. D. Jones,[2] J. Kandaswamy,[2] D. L. Kreinick,[2] V. E. Kuznetsov,[2] H. Mahlke-Krüger,[2] P. U. E. Onyisi,[2] J. R. Patterson,[2] D. Peterson,[2] J. Pivarski,[2] D. Riley,[2] A. Ryd,[2] A. J. Sadoff,[2] H. Schwarthoff,[2] X. Shi,[2] S. Stroiney,[2] W. M. Sun,[2] T. Wilksen,[2] M. Weinberger,[2] S. B. Athar,[3] R. Patel,[3] V. Potlia,[3] J. Yelton,[3] P. Rubin,[4] C. Cawlfield,[5] B. I. Eisenstein,[5] I. Karliner,[5] D. Kim,[5] N. Lowrey,[5] P. Naik,[5] C. Sedlack,[5] M. Selen,[5] E. J. White,[5] J. Wiss,[5] M. R. Shepherd,[6] D. Besson,[7] S. Henderson,[7] T. K. Pedlar,[8] D. Cronin-Hennessy,[9] K. Y. Gao,[9] D. T. Gong,[9] J. Hietala,[9] Y. Kubota,[9] T. Klein,[9] B. W. Lang,[9] R. Poling,[9] A. W. Scott,[9] A. Smith,[9] P. Zweber,[9] S. Dobbs,[10] Z. Metreveli,[10] K. K. Seth,[10] A. Tomaradze,[10] J. Ernst,[11] H. Severini,[12] S. A. Dytman,[13] W. Love,[13] V. Savinov,[13] O. Aquines,[14] Z. Li,[14] A. Lopez,[14] S. Mehrabyan,[14] H. Mendez,[14] J. Ramirez,[14] G. S. Huang,[15] D. H. Miller,[15] V. Pavlunin,[15] B. Sanghi,[15] I. P. J. Shipsey,[15] B. Xin,[15] G. S. Adams,[16] M. Anderson,[16] J. P. Cummings,[16] I. Danko,[16] J. Napolitano,[16] Q. He,[17] J. Insler,[17] H. Muramatsu,[17] C. S. Park,[17] E. H. Thorndike,[17] F. Yang,[17] T. E. Coan,[18] Y. S. Gao,[18] F. Liu,[18] M. Artuso,[19] S. Blusk,[19] J. Butt,[19] J. Li,[19] N. Menaa,[19] G. C. Moneti,[19] R. Mountain,[19] S. Nisar,[19] K. Randrianarivony,[19] R. Redjimi,[19] R. Sia,[19] T. Skwarnicki,[19] S. Stone,[19] J. C. Wang,[19] K. Zhang,[19] S. E. Csorna,[20] G. Bonvicini,[21] D. Cinabro,[21] M. Dubrovin,[21] A. Lincoln,[21] D. M. Asner,[22] K. W. Edwards,[22] R. A. Briere,[23] I. Brock,[23] J. Chen,[23] T. Ferguson,[23] G. Tatishvili,[23] H. Vogel,[23] and M. E. Watkins[23]

(CLEO Collaboration)

[1]*Enrico Fermi Institute, University of Chicago, Chicago, Illinois 60637*
[2]*Cornell University, Ithaca, New York 14853*
[3]*University of Florida, Gainesville, Florida 32611*
[4]*George Mason University, Fairfax, Virginia 22030*
[5]*University of Illinois, Urbana-Champaign, Illinois 61801*
[6]*Indiana University, Bloomington, Indiana 47405*
[7]*University of Kansas, Lawrence, Kansas 66045*
[8]*Luther College, Decorah, Iowa 52101*
[9]*University of Minnesota, Minneapolis, Minnesota 55455*
[10]*Northwestern University, Evanston, Illinois 60208*
[11]*State University of New York at Albany, Albany, New York 12222*
[12]*University of Oklahoma, Norman, Oklahoma 73019*
[13]*University of Pittsburgh, Pittsburgh, Pennsylvania 15260*
[14]*University of Puerto Rico, Mayaguez, Puerto Rico 00681*
[15]*Purdue University, West Lafayette, Indiana 47907*
[16]*Rensselaer Polytechnic Institute, Troy, New York 12180*
[17]*University of Rochester, Rochester, New York 14627*
[18]*Southern Methodist University, Dallas, Texas 75275*
[19]*Syracuse University, Syracuse, New York 13244*
[20]*Vanderbilt University, Nashville, Tennessee 37235*

[21]*Wayne State University, Detroit, Michigan 48202*
[22]*Carleton University, Ottawa, Ontario, Canada K1S 5B6*
[23]*Carnegie Mellon University, Pittsburgh, Pennsylvania 15213*
(Dated: July 26, 2006)

Abstract

Motivated by concerns regarding possible two-body contributions to the recently-measured inclusive $\Upsilon(\mathrm{nS}) \to \gamma + X$ direct photon spectrum, we report on a preliminary new study of exclusive radiative decays of the Υ resonances into two-body final states $\mathcal{R}\gamma$, with $\mathcal{R}$ some resonant hadronic state decaying into four or more charged particles. Such two-body processes are not explicitly addressed in the extant theoretical frameworks used to calculate the inclusive direct photon spectrum. Using data collected from the CLEO III detector at the Cornell Electron Storage Ring, we present upper limits for such $\Upsilon(1\mathrm{S})$, $\Upsilon(2\mathrm{S})$, and $\Upsilon(3\mathrm{S})$ two-body decays as a function of the recoil mass $M_{\mathcal{R}}$. Additionally, we place upper limits on the cross-section for $\mathcal{R}$ production via radiative return for center-of-mass energies just below the $\Upsilon(1\mathrm{S})$, $\Upsilon(2\mathrm{S})$, and $\Upsilon(3\mathrm{S})$ energies. The results presented in this document are preliminary.

*Submitted to the 33rd International Conference on High Energy Physics, July 26 - August 2, 2006, Moscow

Introduction

Very recently, we extracted α_s from a measurement of the direct photon spectra in $\Upsilon(1S, 2S, 3S) \to gg\gamma$ [1]. To extrapolate beyond the experimentally accessible direct photon momentum region, those measurements relied on several theoretical parameterizations of the expected photon momentum spectrum in the Υ system [2, 3] to obtain the total direct $\Upsilon \to gg\gamma$ decay width relative to the dominant $\Upsilon \to ggg$ width. The ratio of those widths can then be used to estimate the strong coupling constant at the energy scale of the Υ. These theoretical parameterizations generally neglect the contribution to the photon momentum spectrum due to two-body decays, e.g. $\Upsilon \to gg\gamma \to \mathcal{R}\gamma$, with $\mathcal{R}$ some resonant hadronic state.

As noted in the α_s extraction, contributions from such possible two-body decays may result in a slight underestimate of the extracted value of α_s. This systematic consideration in the $gg\gamma$ analysis motivated a search for $\Upsilon \to \mathcal{R}\gamma$. We concern ourselves with high multiplicity (≥ 4 charged tracks) final states, as we employ the same hadronic event selection cuts in this analysis that we did in the $gg\gamma$ analysis [1]. We note that, although two-body branching fractions have been observed for, e.g., $\Upsilon(1S) \to \gamma f_2(1270)$ at the level of 10^{-4}, the fraction of $f_2(1270)$ decays into ≥ 4 charged tracks is only $\approx 3\%$ [6]. Our sensitivity to the $f_2(1270)$ is additionally reduced in this analysis by its large width (compared to our typical photon energy resolution).

The analysis, in general terms, proceeds as follows. After selecting a high-quality sample of e^+e^- annihilations into hadrons using the hadronic event selection cuts of the previous analysis [1], we plot the inclusive isolated photon spectrum in data taken at both on-Υ-resonance and off-Υ-resonance energies (the latter sample is used for systematic checks of the overall procedure). A two-body radiative decay of the Υ will produce a monochromatic photon in the lab frame; the momentum of the radiated photon is related to the mass of the recoil hadron $\mathcal{R}$ via Equation 1 ($x_\gamma = E_\gamma / E_{beam}$).

$$M_{\mathcal{R}} = 2E_{beam}\sqrt{1 - (x_\gamma^{\mathcal{R}})^2} \tag{1}$$

Assuming that the intrinsic width of the recoil hadron is much smaller than the experimental photon energy resolution, then the measured radiative photon energy should be a Gaussian centered at the momentum $x_\gamma^{\mathcal{R}}$. For a 1 GeV (4.5 GeV) recoil photon, this implies a recoil mass typically much narrower than 20 MeV (60 MeV). Not knowing *a priori* the mass of the hadron $\mathcal{R}$, we therefore perform a set of fits to the $\Upsilon(1S)$ photon spectrum to a Gaussian signal, centered at the value $x_\gamma^{\mathcal{R}}$, and with a resolution corresponding to the known CLEO-III electromagnetic calorimeter resolution, atop smooth polynomial backgrounds, over the $0.2 < x_\gamma < 1.0$ photon energy range. [1]

We construct 95% confidence level upper limits from these fits by adding $1.645 * \sigma_A(x_\gamma)$ to the $A(x_\gamma)$ distribution, where $A(x_\gamma)$ is the x_γ-dependent Gaussian fit area and $\sigma_A(x_\gamma)$ is the fit error. We then recast this upper limit as a function of recoil mass $M_{\mathcal{R}}$, correct for

[1] It should be noted that 'bumps' in the inclusive photon spectrum can be due not only to resonant two-body decays but also to continuum threshold effects like the crossing of the $c\overline{c}$ threshold. In the previous analysis, we also identified an excess of photons in data as $x_\gamma \to 1$. Further examination of these events indicated that they were dominated by $e^+e^- \to \gamma\pi^+\pi^-\pi^+\pi^-$, although the possibility that the 4-pion state resulted from the decay of an intermediate resonance $\mathcal{R}$ was not investigated.

the efficiency loss due to the fiducial acceptance of the detector (for the purposes of this correction, it is assumed that $\mathcal{R}$ is pseudo-scalar with a corresponding $1 + \cos^2\theta$ angular distribution for the recoiling γ) and of the event and photon selection cuts that define our data sample. Note that the exact form of the efficiency correction due to the event and photon selection cuts varies with the decay final states considered for $\mathcal{R}$. To be conservative, we derive our x_γ-dependent efficiency correction from the decay mode yielding the lowest reconstruction efficiency imaginable.

This final efficiency-corrected limit is converted into an $M_{\mathcal{R}}$-dependent branching ratio upper limit $\mathcal{B}(\gamma\mathcal{R})$ by dividing the resulting yield by the calculated total number of resonant Υ events. For the off-resonance running, the distributions are divided by the off-resonance luminosity for comparison's sake. An example of simulated signal superimposed on background is given in Figure 1 for $\Upsilon(4S) \to \gamma + \mathcal{R}$, $\mathcal{R} \to \pi^+\pi^-\pi^+\pi^-$.

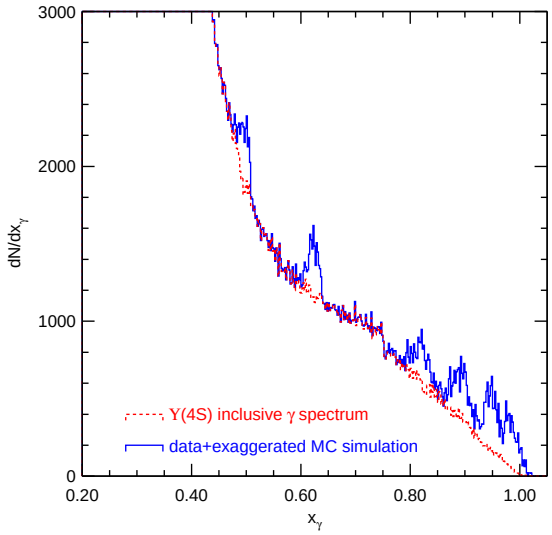

FIG. 1: $\Upsilon(4S) \to \mathcal{R}\gamma$, $\mathcal{R} \to 4\pi$, for various hypothetical $\mathcal{R}$ masses. The magnitude of $\mathcal{B}(\Upsilon(4S) \to \mathcal{R}\gamma,\ \mathcal{R} \to 4\pi)$ has been grossly exaggerated for the sake of presentation. The red (dotted) curve is $\Upsilon(4S)$ data, while the blue (solid) curve is $\Upsilon(4S)$ data with signal Monte Carlo added on top. From the left, the first 'bump' corresponds to a $\mathcal{R}$ of mass $\approx$ 7.6 GeV, the second from the left corresponds to a $\mathcal{R}$ of mass $\approx$ 6.5 GeV, the third from the left corresponds to a $\mathcal{R}$ of mass $\approx$ 4.7 GeV and the fourth from the left corresponds a $\mathcal{R}$ of mass $\approx$ 3.3 GeV.

Event Selection

Event selection criteria in this analysis are identical to those imposed in the previous analysis [1]. The inclusive photon spectra are therefore identical to those taken from our previous analysis, as well. The background shape is approximately exponential in the region from $0.2 < x_\gamma < 1.0$.

Fitting the Inclusive Photon Spectrum

To extract the possible magnitude of a two-body radiative signal, we step along the inclusive photon spectrum over the interval $0.2 < x_\gamma < 1.0$, fitting it to a Gaussian with width equal to the detector resolution at that value of photon energy, plus a background parametrized by a smooth Chebyshyev polynomial. We assume that the intrinsic width of the resonance $\mathcal{R}$ is considerably smaller than the detector resolution. Our step size is determined by the energy resolution of the detector $\sigma_{\rm E}$; we use steps of width $\sigma_{\rm E}/2$. For photons in the central "barrel" region of the CsI electromagnetic calorimeter, at energies greater than 2 GeV, the energy resolution is given by

$$\frac{\sigma_{\rm E}}{E}(\%) = \frac{0.6}{E^{0.73}} + 1.14 - 0.01E, \tag{2}$$

where E is the shower energy in GeV. At 100 MeV, the calorimetric performance is about 20% poorer than indicated by this expression due to the material in front of the calorimeter itself.

At each step, we use a $\pm 10\sigma_{\rm E}$ fitting window; the background is expected to be relatively smooth over such a limited interval. We use a 3rd-(2nd-)order Chebyschev polynomial in the photon interval $x_\gamma < (>) 0.6$. For each fit, the Gaussian fit area $A(x_\gamma)$ and fit error $\sigma_A(x_\gamma)$ is recorded. Note that the fits are highly correlated point-to-point, and that the bin width is much finer than the detector resolution. Note also that we have not attempted to analytically correct for smearing-induced distortions that may result from the finite resolution of the detector; we simply assume that the smeared spectrum can be well-described by a smooth higher-order polynomial.

Extracting Upper Limits

To convert the $A(x_\gamma)$ distribution obtained from fitting the inclusive photon spectrum into a one-sided upper 95% confidence interval upper limit, we add $1.645 * \sigma_A(x_\gamma)$ point-wise to the $A(x_\gamma)$ distribution, as a function of photon momentum. In this process, since we are interested in enhancements in the inclusive photon spectrum, all negative areas from the raw fits are set equal to $1.645 * \sigma_A(x_\gamma)$ at these points. The resulting contour for the $\Upsilon(1S)$ fitting is shown in Figure 2.

We convert the limits as a function of photon energy x_γ into a function of a hypothetical resonance recoil mass $M_{\mathcal{R}}$ via Equation 1. For the purposes of this conversion the mean values for each running period of E_{beam} are used for each data sample; we neglect the MeV-scale variation in beam energies for a particular run period. These values are given in Table I.

The resulting $M_{\mathcal{R}}$-dependent contour, for the $\Upsilon(1S)$, is shown in Figure 3.

Efficiency Correction

We consider two efficiency corrections to the upper limit contour: one due to the fiducial acceptance of the detector, and the other due to our event and shower selection cuts.

For photons in the "barrel" of the detector ($|\cos\theta| < 0.707$, with θ the polar angle of the photon momentum relative to the beam axis), we assume that $\mathcal{R}$ is a pseudo-scalar,

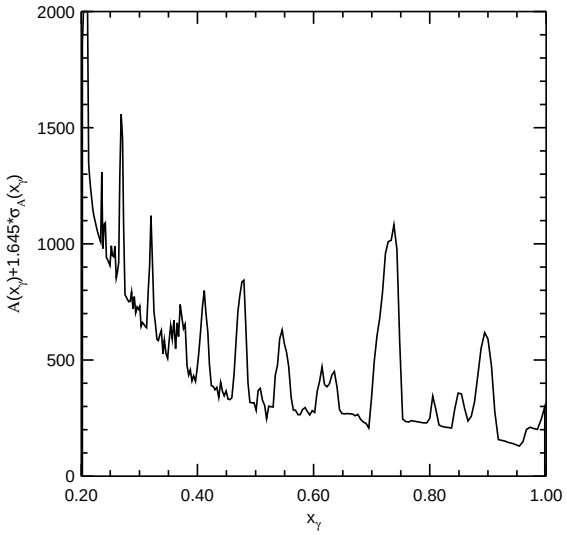

FIG. 2: $A(x_\gamma) + 1.645 * \sigma_A(x_\gamma)$ versus x_γ for fits to the $\Upsilon(1S)$ inclusive photon spectrum, where negative points have been mapped to $1.645 * \sigma_A(x_\gamma)$.

Event Type	Average Beam Energy ($\overline{E_{beam}}$)
Resonance $\Upsilon(1S)$	4.73 GeV
Resonance $\Upsilon(2S)$	5.01 GeV
Resonance $\Upsilon(3S)$	5.18 GeV
Continuum $\Upsilon(1S)$	4.72 GeV
Continuum $\Upsilon(2S)$	5.00 GeV
Continuum $\Upsilon(3S)$	5.16 GeV
Continuum $\Upsilon(4S)$	5.27 GeV

TABLE I: The mean values of E_{beam} for each data sample used in this analysis, used to map our upper limit contour from a function of x_γ to a function of $M_{\mathcal{R}}$.

which corresponds to a $1 + \cos^2\theta$ distribution on the photons in the two-body decays we are considering. This choice is arbitrary and amounts to an ≈ 0.6 uniform acceptance efficiency correction to our limit. In addition to this angular acceptance correction, we assess an efficiency correction due to the CLEO III detection efficiency. Not knowing *a priori* what the decay mode of our hypothetical resonance $\mathcal{R}$ will be, we have generated 5000-event Monte Carlo samples spanning a wide range of final state charged (and neutral) multiplicities and masses $M_{\mathcal{R}}$. In the interests of producing a conservative upper limit, we take our efficiency correction from the mode which yields the lowest average efficiency in the main $M_{\mathcal{R}}$ interval of interest. A list of $\mathcal{R}$ decay modes considered in this analysis and their average efficiencies (averaged over the photon momentum spectrum from 1.0 GeV $\leq E_\gamma \leq$ 4.5 GeV) is given in Table II. We thereby derive a collection of efficiency measurements distributed over photon momentum E_γ, each of which corresponds to a different hypothesis for the mass $M_{\mathcal{R}}$. To obtain efficiencies between these points (where we have not explicitly filled in the efficiency

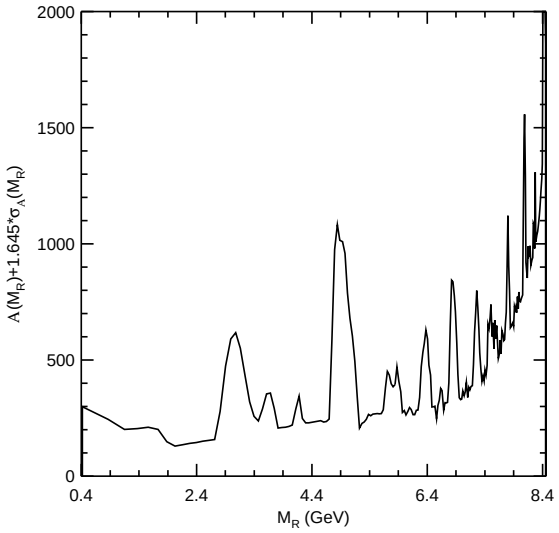

FIG. 3: $A(M_{\mathcal{R}}) + 1.645 * \sigma_A(M_{\mathcal{R}})$ versus $M_{\mathcal{R}}$ for fits to the $\Upsilon(1S)$ inclusive photon spectrum. This curve was obtained from mapping the points in Figure 2 into recoil mass space via Equation 1

with a $M_{\mathcal{R}}$ hypothesis), we perform a linear extrapolation between the two neighboring points. In this manner, we point-wise efficiency correct our upper limit as a function of x_γ (or E_γ) before mapping the upper limit into $M_{\mathcal{R}}$. We find that the lowest efficiency for various hypothetical decay modes of $\mathcal{R}$ considered was obtained from $\mathcal{R} \to 4K\pi^0$ (Figure 4). We therefore use this efficiency function to determine our upper limit contours.

Results

To convert the efficiency corrected upper limit contour into an upper limit on the two-body radiative branching ratio $\mathcal{B}(\gamma\mathcal{R})$, we simply divide the efficiency-corrected upper limit contour by the total calculated number of $\Upsilon(1S)$, $\Upsilon(2S)$ and $\Upsilon(3S)$ events. These numbers were calculated in our previous analysis [1], and for convenience are reproduced in Table III. For comparison's sake, the efficiency-corrected upper limit contours obtained from fitting below Υ resonance data have been divided by the total luminosity of off-resonance data taking and therefore correspond to an upper limit on a cross-section. The resulting on-resonance upper limit $\mathcal{B}(\gamma\mathcal{R})$ is shown in Figure 5, and the resulting off-resonance cross-section "limit" is shown in Figure 6. To set the scale of the continuum cross-section limits, the raw ISR cross-section for $e^+e^- \to \psi + \gamma$ is expected to be $\sim$5 pb in the 10 GeV center-of-mass regime, implying an expected observed cross-section into $\geq$4 charged tracks $\sim 10^{-4}$ nb, taking into account the strong forward peaking expected for ISR processes.

Given the fact that we have not performed a continuum subtraction on the on-resonance inclusive photon spectrum from Υ decays, it is interesting to compare the structure observed in Figure 5 with structure observed when we apply the fitting procedure to continuum data. Figures 7, 8 and 9 show the resonances limits of Figure 5 separately, with the respective continuum limits of Figure 6 overlaid for comparison. We observe some, albeit not complete,

Event Type	Average Efficiency ($\overline{\epsilon}$)
$\mathcal{R} \to K^+K^-\pi^+\pi^-$	0.53 ± 0.03
$\mathcal{R} \to K^+K^-\pi^+\pi^-\pi^0$	0.53 ± 0.02
$\mathcal{R} \to K^+K^-\pi^+\pi^-\pi^0\pi^0$	0.54 ± 0.02
$\mathcal{R} \to K^+K^-p^+p^-$	0.56 ± 0.02
$\mathcal{R} \to K^+K^-p^+p^-\pi^0$	0.50 ± 0.05
$\mathcal{R} \to K^+K^-p^+p^-\pi^0\pi^0$	0.57 ± 0.02
$\mathcal{R} \to p^+p^-\pi^+\pi^-$	0.62 ± 0.03
$\mathcal{R} \to p^+p^-\pi^+\pi^-\pi^0$	0.54 ± 0.05
$\mathcal{R} \to p^+p^-\pi^+\pi^-\pi^0\pi^0$	0.63 ± 0.02
$\mathcal{R} \to K^+K^-K^+K^-$	0.50 ± 0.02
$\mathcal{R} \to K^+K^-K^+K^-\pi^0\pi^0$	0.49 ± 0.02
$\mathcal{R} \to p^+p^-p^+p^-$	0.67 ± 0.02
$\mathcal{R} \to p^+p^-p^+p^-\pi^0$	0.65 ± 0.02
$\mathcal{R} \to p^+p^-p^+p^-\pi^0\pi^0$	0.63 ± 0.02
$\mathcal{R} \to \pi^+\pi^-\pi^+\pi^-$	0.59 ± 0.02
$\mathcal{R} \to \pi^+\pi^-\pi^+\pi^-\pi^0$	0.65 ± 0.02
$\mathcal{R} \to \pi^+\pi^-\pi^+\pi^-\pi^0\pi^0$	0.59 ± 0.01
$\mathcal{R} \to \pi^+\pi^-\pi^+\pi^-4\pi^0$	0.57 ± 0.02
$\mathcal{R} \to \pi^+\pi^-\pi^+\pi^-6\pi^0$	0.60 ± 0.02
$\mathcal{R} \to \pi^+\pi^-\pi^+\pi^-8\pi^0$	0.60 ± 0.02
$\mathcal{R} \to K^+K^-K^+K^-K^+K^-$	0.68 ± 0.04
$\mathcal{R} \to p^+p^-p^+p^-p^+p^-$	0.53 ± 0.04
$\mathcal{R} \to \pi^+\pi^-\pi^+\pi^-\pi^+\pi^-$	0.74 ± 0.03
$\mathcal{R} \to K^+K^-K^+K^-\pi^0$	**0.48 ± 0.02**

TABLE II: Average efficiencies for the reconstruction of various events that could be detected in this analysis, obtained by fitting the photon momentum-dependent reconstruction efficiencies to a straight line in the interval 1.0 GeV $< E_\gamma <$ 4.5 GeV. The presented errors on the efficiencies are statistical only. The lowest-efficiency final state ($K^+K^-K^+K^-\pi^0$) is used for setting upper limits.

correlation between the two.

Υ Resonance	$N_{\rm total}(\Upsilon({\rm nS}))$ ($\times 10^6$)
Υ(1S)	21.0 ± 0.06
Υ(2S)	8.4 ± 0.04
Υ(3S)	5.2 ± 0.06

TABLE III: The total number of calculated Υ(1S), Υ(2S) and Υ(3S) events in our data samples [1].

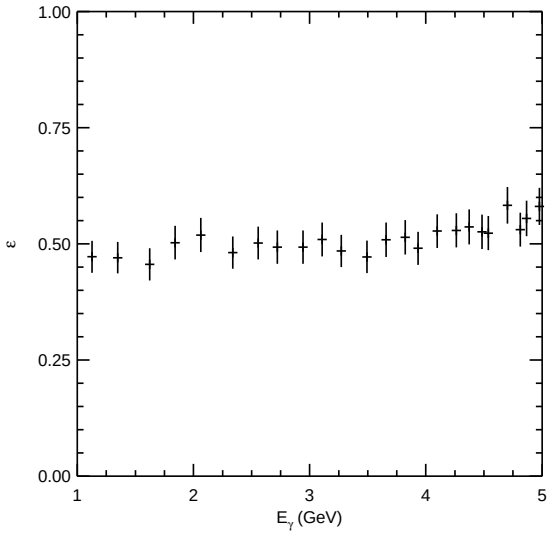

FIG. 4: The efficiency for detecting an $\Upsilon \to \gamma + \mathcal{R}$, $\mathcal{R} \to 4K\pi^0$ event as a function of observed photon energy E_γ. Each point in this efficiency is obtained from a different $\mathcal{R}$ mass hypothesis. This photon momentum-dependent efficiency correction distribution is used to point-wise correct our upper limit, where the efficiency between points in this distribution is estimated by linear interpolation.

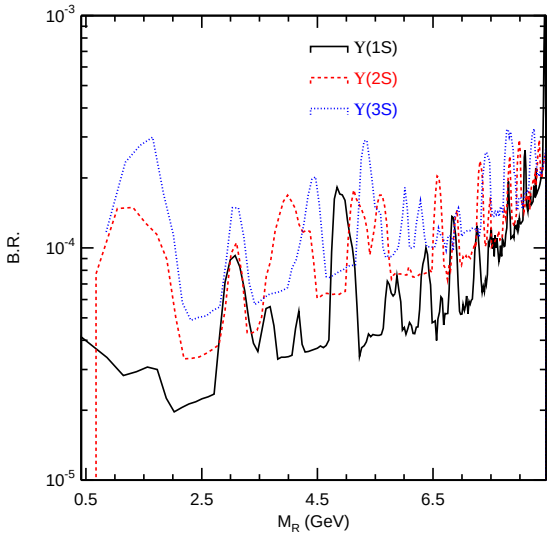

FIG. 5: The $M_{\mathcal{R}}$-dependent $\mathcal{B}(\gamma\mathcal{R})$ upper limit contours obtained for $\Upsilon \to \gamma + \mathcal{R}$, $\mathcal{R} \to \geq 4$ charged tracks for the $\Upsilon(1S)$, $\Upsilon(2S)$ and $\Upsilon(3S)$. All limits are of order $\mathcal{B}(\gamma\mathcal{R}) \approx 10^{-4}$.

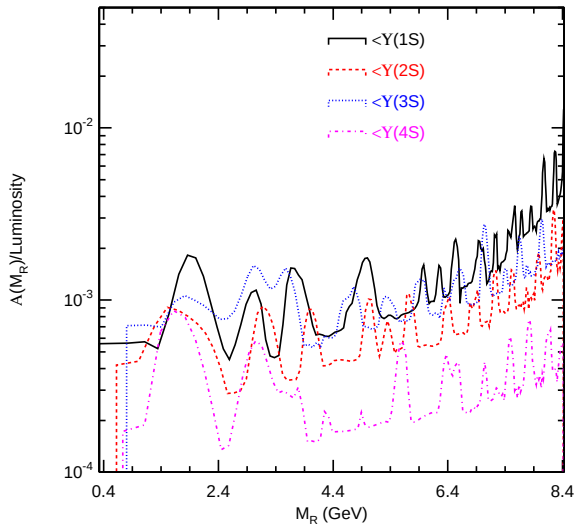

FIG. 6: Our $M_{\mathcal{R}}$-dependent cross-section upper limit contours obtained for $e^+e^- \to \gamma+\mathcal{R}$, $\mathcal{R} \to \geq 4$ charged tracks for the continua below $\Upsilon(1S)$, $\Upsilon(2S)$, $\Upsilon(3S)$ and $\Upsilon(4S)$ (nb). This plot is obtained by dividing the result of our fitting procedure on the continuum by the off-resonance luminosity. The angular correction here is (as before) $1 + \cos^2\theta_\gamma$.

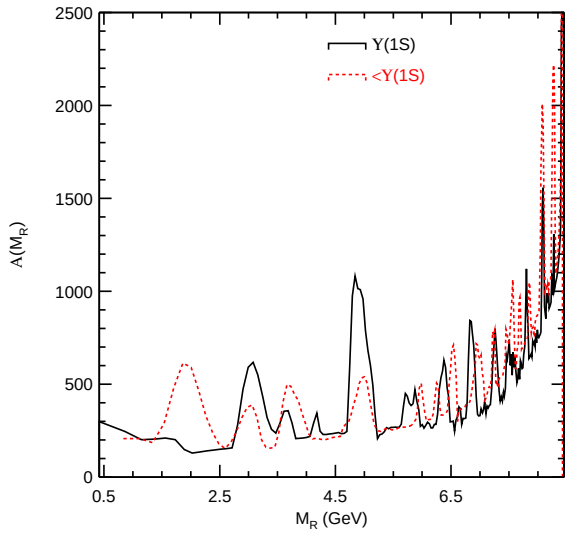

FIG. 7: Comparison of the $M_{\mathcal{R}}$-dependent Gaussian fit area $A(M_{\mathcal{R}})$ for the $\Upsilon(1S)$ versus the continuum below $\Upsilon(1S)$. Note the correlation between the resonance and the below-resonance structure. Note also that the below-resonance upper limit curve has been scaled to match the 'floor' of the on-resonant upper limit curve.

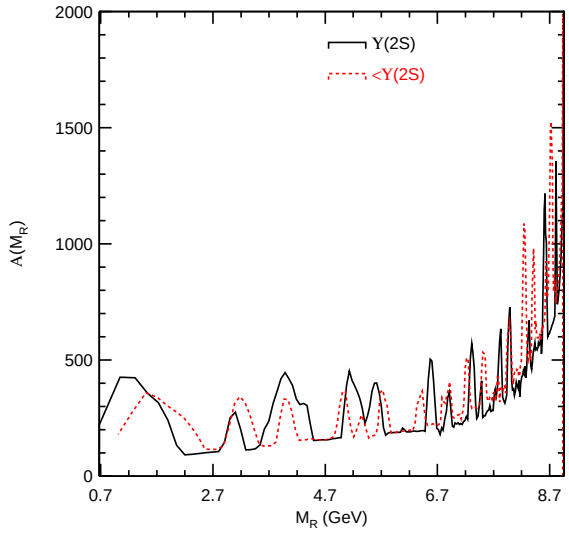

FIG. 8: Comparison of the $M_{\mathcal{R}}$-dependent Gaussian fit area $A(M_{\mathcal{R}})$ for the $\Upsilon(2S)$ versus the continuum below $\Upsilon(2S)$. Note that the below-resonance upper limit curve has been scaled to match the 'floor' of the on-resonant upper limit curve.

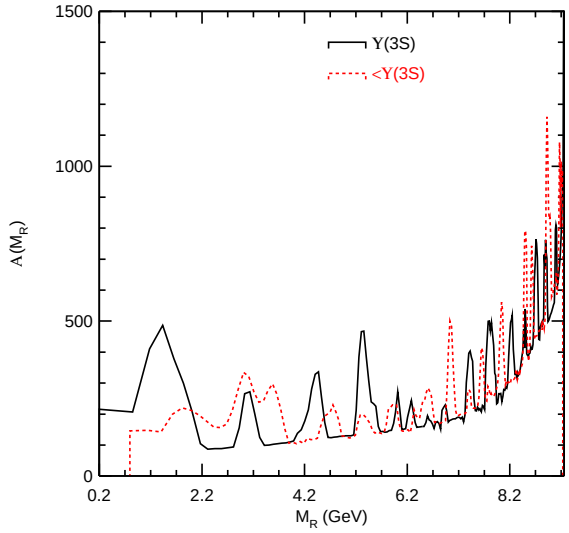

FIG. 9: Comparison of the $M_{\mathcal{R}}$-dependent Gaussian fit area $A(M_{\mathcal{R}})$ for the $\Upsilon(3S)$ versus the continuum below $\Upsilon(3S)$. Note that the below-resonance upper limit curve has been scaled to match the 'floor' of the on-resonant upper limit curve.

Cross-Check

In order to ensure that we are able to identify a signal at a given sensitivity level, we embedded pure Monte Carlo signal in data, and performed our fitting procedure on the resulting distribution in order to ensure that we recovered the correct signal magnitude in our branching ratio upper limit. To do this, $\Upsilon(4S) \to \gamma + \mathcal{R}$, $\mathcal{R} \to \pi^+\pi^-\pi^+\pi^-$ events were embedded in the $\Upsilon(4S)$ inclusive photon spectrum with branching ratios of the order of 10^{-5}, 10^{-4}, 10^{-3}, and 10^{-2}, under 10 different $M_{\mathcal{R}}$ hypotheses: $M_{\mathcal{R}} = 0.6$ GeV, 1.5 GeV, 2.5 GeV, 3.5 GeV, 4.5 GeV, 6.5 GeV, 7.5 GeV, 8.5 GeV, 9.5 GeV and 10.5 GeV. The resulting upper limit contours derived from applying our procedure to these spectra are show in Figure 10. We reconstruct all signals above our upper limit floor (around 10^{-4}) that are within our accessible recoil mass range.

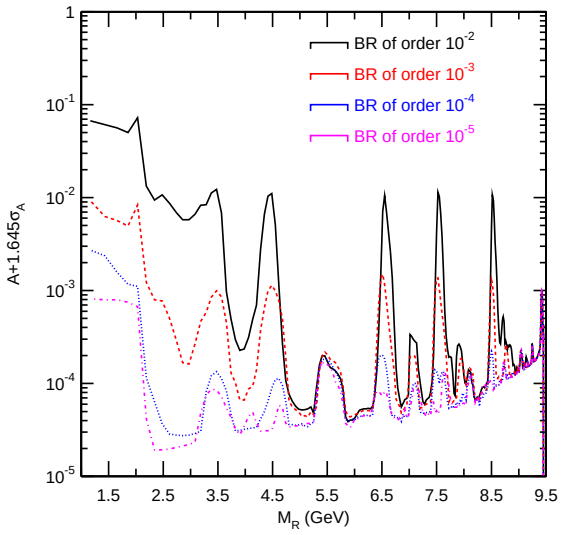

FIG. 10: Upper limit contours derived from applying our procedure to fabricated Monte Carlo signal spectra. We reconstruct all input signals above our upper limit floor ($\approx 10^{-4}$) that are within our accessible recoil mass range.

Systematic errors

We identify and account for systematic errors as follows:

1. We account for possible systematics in our event and shower reconstruction efficiency by using the lowest-efficiency final state considered.

2. We assess a uniform 1% degradation of the limit due to the luminosity uncertainty as calculated in the previous analysis [1].

3. We degrade the limit uniformly by the uncertainty in the calculated number of total $\Upsilon(1S)$, $\Upsilon(2S)$ and $\Upsilon(3S)$ events.

Summary

As shown in Figure 5, our sensitivity is of order 10^{-4} across all possible values of $M_{\mathcal{R}}$, well above the threshold for any known branching ratio for $\Upsilon \to \gamma$+pseudoscalar, pseudoscalar$\to$ $h^+h^-h^+h^-$+neutrals. We measure upper limits of $\mathcal{B}(\Upsilon(1S) \to \gamma + \mathcal{R}, \mathcal{R} \to \geq 4$ charged tracks $) < 1.05 \times 10^{-3}$, $\mathcal{B}(\Upsilon(2S) \to \gamma + \mathcal{R}, \mathcal{R} \to \geq 4$ charged tracks $) < 1.65 \times 10^{-3}$ and $\mathcal{B}(\Upsilon(3S) \to \gamma + \mathcal{R}, \mathcal{R} \to \geq 4$ charged tracks $) < 2.47 \times 10^{-3}$ for all possible masses $M_{\mathcal{R}}$, under the assumption that $\mathcal{R}$ is a pseudoscalar. Constraining 1.5 GeV $< M_{\mathcal{R}} <$ 5.0 GeV we set a much more stringent limit of $\mathcal{B}(\Upsilon(1S) \to \gamma + \mathcal{R}, \mathcal{R} \to \geq 4$ charged tracks $) < 1.82 \times 10^{-4}$, $\mathcal{B}(\Upsilon(2S) \to \gamma + \mathcal{R}, \mathcal{R} \to \geq 4$ charged tracks $) < 1.69 \times 10^{-4}$ and $\mathcal{B}(\Upsilon(3S) \to \gamma + \mathcal{R}, \mathcal{R} \to \geq 4$ charged tracks $) < 3.00 \times 10^{-4}$. Additionally, we report these upper limits as a function of the mass recoiling against the photon, as shown in Figure 5. We also report cross-section limits for resonant processes on the continuum (Figure 6).

We note that we appropriately ignored the distortion of the inclusive photon spectrum in our previous extraction of α_s due to two-body decays as we limit the branching ratio of these events to be $\leq 10^{-4}$. Further work on exclusive multiparticle final states (e.g., $\gamma 4\pi$, $\gamma 4K$, $\gamma K^0 K^0$ and $\gamma K^0 K \pi$) would help elucidate the nature of such radiative decays.

Acknowledgments

We gratefully acknowledge the effort of the CESR staff in providing us with excellent luminosity and running conditions. D. Cronin-Hennessy and A. Ryd thank the A.P. Sloan Foundation. This work was supported by the National Science Foundation, the U.S. Department of Energy, and the Natural Sciences and Engineering Research Council of Canada.

---

[1] D. Besson *et al.* (CLEO Collaboration), arXiv:hep-ex/0512061, accepted by Phys. Rev. D.

[2] R.D. Field, Phys. Lett. **B133**, 248 (1983).

[3] X. Garcia and J. Soto, Phys. Rev. Lett. **96**, 111801 (1996).

[4] S. B. Athar *et al.* (CLEO Collaboration), arXiv:hep-ex/0510015, Phys. Rev. **D73**, 032001 (2006).

[5] D. Besson *et al.* (CLEO Collaboration), arXiv:hep-ex/0512003, submitted to Phys. Rev. D.

[6] S. Eidelman *et al.* (Particle Data Group), Phys. Lett. B **592**, 1 (2004)

[7] Y. Kubota *et al.* (CLEO Collaboration), Nucl. Inst. Meth. **A 320**, 66 (1992).

[8] D. Peterson *et al.*, Nucl. Inst. Meth. **A 478**, 142 (2002).

[9] M. Artuso *et al.*, Nucl. Inst. Meth. **A 502**, 91 (2003).